

2. Materials and methods

2.1. Materials

The clathrochelates were prepared as described elsewhere.³⁵ BSA and HSA were obtained commercially (fraction V from Sigma-Aldrich® and fraction V protease free from Fisher Bioreagents®, respectively). 0.05 M Tris-HCl aqueous buffer (pH 7.9), 0.05 M aqueous phosphate buffers (pH 5 and pH 6), and 0.05 M aqueous acetate buffer (pH 3.7) were used as solvents.

2.2. Preparation of the solutions for protein fluorescence quenching studies

Aqueous solutions of BSA and HSA (concentration of 0.2 mg ml⁻¹ – 3 μM) were prepared by dissolution of their weighed amounts in corresponding buffer. 2 mM stock DMSO solutions of the clathrochelates were prepared, and an aliquot was added to Tris-HCl buffer solution of a chosen protein. Since the amount of added DMSO solution was rather small (up to 2.5% of the total volume), the protein's concentration remained practically unchanged (0.2 mg ml⁻¹), while that of the clathrochelate changed from 0 to 15 μM.

2.3. Fluorescence assay

To study the quenching of albumin fluorescence upon the binding of iron(II) clathrochelates, the fluorescence spectra of the protein itself and after the addition of a DMSO solution of clathrochelate were recorded. Albumin fluorescence was excited at 280 and 295 nm, and the signal was recorded at λ_{max} of corresponding emission. Fluorescence spectra were measured at 5 nm width of the excitation and emission slits at room temperature on a Cary Eclipse fluorescence spectrophotometer (Varian) in a 1 cm × 1 cm quartz cell. To avoid possible errors caused by differences in the media used for the fluorescent and ITC experiments (Tris-HCl aqueous buffer and sodium acetate aqueous solution, respectively), fluorescence quenching measurements were also performed in sodium acetate aqueous solution. The observed differences were found to be insignificant.

An increase in the clathrochelate concentration led to the simultaneous increase in the optical density at maxima of BSA excitation and/or emission, thus causing a decrease of observed fluorescence intensity because of the so-called “inner filter effect” (IFE), as well as due to the reabsorption process.^{36,37} These effects should be taken into account for the correct interpretation of the experimental data.^{37–39} The correction factor for these effects can be calculated using eqn (1):³⁹

$$I_{\text{COR}} = I_{\text{OBS}} \times 10^{(D_{\text{EX}} + D_{\text{EM}})/2} \quad (1)$$

where I_{COR} and I_{OBS} are the corrected and observed fluorescence intensities, respectively; D_{EX} and D_{EM} are the total optical densities of a solution at the wavelengths of the fluorescence excitation and emission, respectively. All the experimental fluorescent data were corrected using eqn (1).

2.4. UV-vis spectroscopy

The UV-vis absorbance spectra of BSA-clathrochelate assemblies were recorded at room temperature on a Specord M-40

spectrophotometer (Carl Zeiss, Germany). An aliquot of 2 mM stock DMSO solution of the cage complex was added to 0.05 M Tris-HCl aqueous buffer solution, pH 7.9. The concentration of clathrochelate was varied from 0 to 15 μM.

2.5. ICD spectroscopy

The CD spectra were recorded on a Jasco J-1500 spectropolarimeter at room temperature in the 300–600 nm range, in 0.1 nm steps with a scan of 3001 points; three scans were averaged for each of the ICD spectra. The data expressed as ellipticity (mdeg) were obtained in mdeg units directly from the instrument. Tris-HCl aqueous buffer (pH 7.9), phosphate aqueous buffers (pH 5 and pH 6) and acetate aqueous buffer (pH 3.7) were used for the preparation of stock solutions of the proteins as well as for working solutions with an albumin-to-clathrochelate 2:1 molar ratio ($c_{\text{albumin}} = 8 \times 10^{-5} \text{ mol l}^{-1}$, $c_{\text{clt}} = 4 \times 10^{-5} \text{ mol l}^{-1}$). It should be mentioned that the observed fluorescence quenching is rather low at such a molar ratio. But due to the peculiarities of the experiment (higher sensitivity of the fluorescence method compared to the CD method), absolute concentrations used in CD studies were much higher as compared to the ones used in fluorescence studies (albumin concentration equals $8 \times 10^{-5} \text{ mol l}^{-1}$ and $3 \times 10^{-6} \text{ mol l}^{-1}$ respectively). Thus, a significantly higher percentage of clathrochelate molecules is bound to albumins at a 2:1 molar ratio for the conditions of the CD experiment, and induced CD was clearly observed.

The clathrochelate binding site was evaluated by displacement of clathrochelate upon addition of site markers: (i) warfarin,^{3,41} and (ii) ibuprofen.¹³ A 50-fold excess ($2 \times 10^{-3} \text{ M}$) of warfarin or ibuprofen was added to a mixture of protein ($c_{\text{albumin}} = 8 \times 10^{-5} \text{ mol l}^{-1}$) and clathrochelate ($c_{\text{clt}} = 4 \times 10^{-5} \text{ mol l}^{-1}$).

2.6. ITC experiments

A 5 mM solution of clathrochelate in 0.15 M aqueous sodium acetate was added to a 0.5 mM solution of BSA in 0.15 M aqueous sodium acetate thus obtaining a working solution with clathrochelate-to-protein molar ratios from 0 to 3. ITC experiments were carried out on a Nano ITC calorimeter (TA Instruments), equipped with a standard 1.0 ml cell (24K Gold). The stock solution of clathrochelate was added to the cell using a 250 μl syringe. The calorimetric experiments were operated by Nano ITC Run v. 2.2.3 software. All the experimental data were evaluated using the NanoAnalyze v. 2.4.1 program package and an independent model was used for their interpretation. In each case, control experiments were performed and the enthalpies of dilution of the components were subtracted from the data for their supramolecular assembly.

3. Results and discussion

3.1. Supramolecular binding of the hexacarboxyl-terminated iron(II) clathrochelates to BSA and HSA

BSA and HSA are heart-shaped proteins, the crystal structures of which are very similar.⁴¹ The molecule of HSA consists of three helical domains (I, II and III), each comprising two





Fig. 1 Structure of the albumin molecule (adopted from ref. 48).

subdomains (A and B; Fig. 1). The drug binding **site 1** (Sudlow's I) is a binding pocket within a core in the subdomain **IIA**. Drug binding **site 2** (Sudlow's II) is located in subdomain **IIIA**.^{42–44} Despite the similarity of BSA and HSA molecular structures, the proteins possess certain regions with substantial differences in amino acid sequences;⁴⁵ the BSA molecule was reported to be less conformationally flexible than HSA.⁴⁶

The type of serum albumin, BSA *versus* HSA, was shown to affect the association of various drugs/toxins, such as warfarin, ochratoxin A and phenylbutazone,^{46,47} with **site 1**, *i.e.* the stability constants and competing capacity. The structural distinctions between the binding sites of BSA and HSA are suggested to cause variations of the ICD output of clathrochelates upon their association.

3.1.1. Protein fluorescence quenching studies. The effect of clathrochelates on BSA and HSA fluorescence was studied to characterize the BSA/HSA–clathrochelate host–guest assemblies. The Stern–Volmer plots of protein fluorescence quenching intensities *versus* the clathrochelate-to-protein molar ratio are shown in Fig. 2.

The quenching of proteins' intrinsic fluorescence observed in the presence of clathrochelate compounds (Fig. 2 and Fig. S1a–i, ESI[†]) evidenced the formation of their host–guest supramolecular associates. The fluorescence intensity was much more affected by clathrochelate addition in the case of BSA (6.9–7.5-fold quenching, Fig. 2a) than in that of HSA (2–2.4-fold quenching, Fig. 2c). Shifts of the corresponding emission maxima (up to 20 nm to the short-wavelength range for BSA, and up to 9 nm to the long-wavelength range for HSA) were observed (Fig. S1 and S2, ESI[†]).

Tryptophan (Trp) residues are the brightest fluorophores in albumin, and characteristics of Trp emission (the emission intensity and maximum) are sensitive to the surrounding medium.^{49,50} Apart from Trp, also tyrosine (Tyr) residues contribute to the intrinsic fluorescence of proteins;⁵¹ BSA and HSA contain twenty and eighteen Tyr residues per protein macromolecule, respectively.^{2,41} However, in comparison to Trp, the fluorescence of Tyr residues is less intense and independent of the local environment.

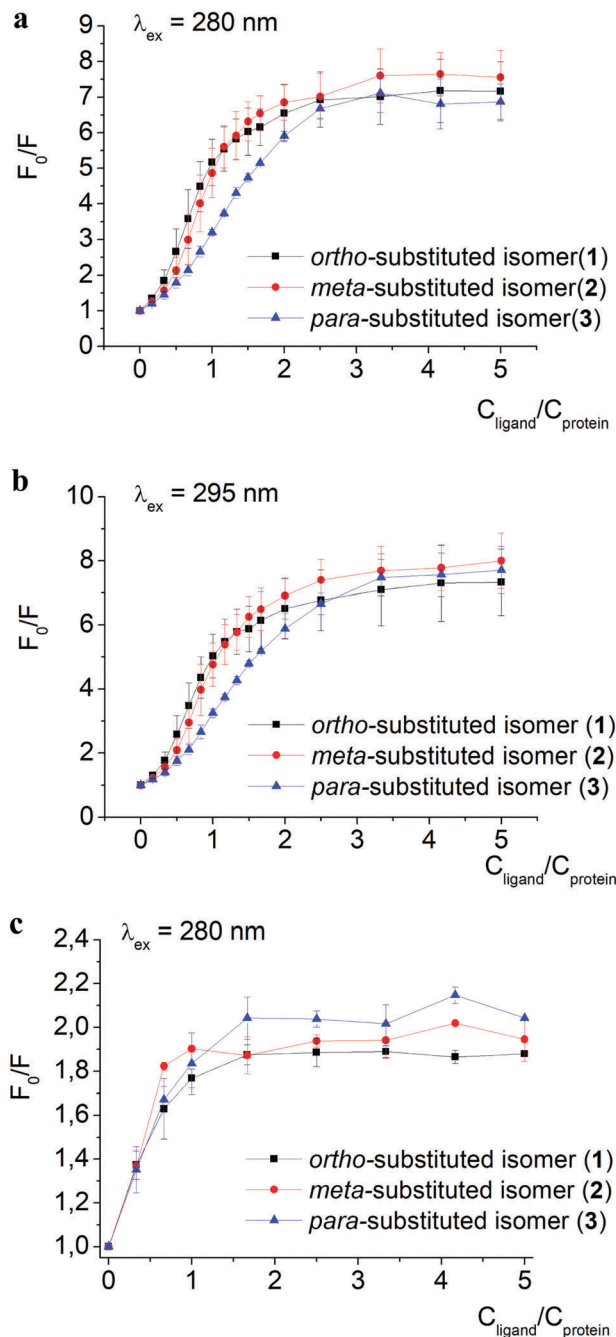


Fig. 2 Stern–Volmer plots of fluorescence intensity quenching of BSA emission excited at 280 (a) and 295 (b) nm, as well as of HSA emission excited at 280 nm (c), by clathrochelates **1–3**; F_0 and F are protein fluorescence intensities in the absence and in the presence of these complexes. Spectra were recorded in 0.05 M Tris HCl, pH 7.9.

A weak effect of fluorescence quenching and a small shift of the emission maximum observed upon iron(II) clathrochelate binding to HSA might be explained by the low accessibility of the single Trp-214 residue that is hidden within a protein globule (subdomain **IIA**). On the other hand, the BSA macromolecule contains two Trp residues: surface-located Trp-134 (subdomain **IB**), and pocket-buried Trp-213 (subdomain **IIA**, Fig. 1).⁵⁰ The efficiency of BSA fluorescence quenching by



hexacarboxyphenylsulfide iron(II) clathrochelates is similar to that of the *ortho*- and *para*-isomers of di-substituted macrobicyclic analogs, but is smaller than that caused by binding of the di-*meta*-substituted cage complex.^{31,50}

The Stern–Volmer plots for BSA–clathrochelate assemblies (Fig. 2a and b) suggest that *ortho*- and *meta*-isomers (complexes 1 and 2, respectively) possess similar fluorescence quenching patterns (with a bend of the corresponding curves at a clathrochelate-to-BSA 3:2 molar ratio), while for *para*-substituted analog 3 the increase is more gradual (with a bend at a molar ratio of approximately 3:1). For HSA, the quenching patterns for iron(II) clathrochelate isomers are of similar shape (Fig. 2c and Fig. S3, ESI†) with the bend values close to a 1:1 molar ratio. The observed behavior could be explained by “multiple quenching” of two Trp residues in BSA, and “single” quenching of one Trp residue in HSA.

To estimate the effect of the clathrochelate binding on the fluorescence of both Trp and Tyr amino acids, we performed quenching experiments (Fig. 2a–c and Fig. S3, ESI†) upon excitation at 280 nm, where both Trp and Tyr are excited, and at 295 nm where only Trp residues are excited.⁴⁹ The data clearly show similar quenching patterns upon both used excitation wavelengths for clathrochelate assemblies with BSA or HSA. This indicates that the binding of clathrochelates to albumins quenches mainly Trp emission, and only slightly that of Tyr residues.

Thus we suggest that the quenching of albumin fluorescence is caused by the binding of clathrochelates near Trp-213 and Trp-134 of BSA, or Trp-214 of HSA; the binding most probably occurs at **site 1** located in protein subdomain **IIA**.

3.1.3. ICD sensing of the “relative structure” of albumins using clathrochelates. The binding of the hexacarboxyphenylsulfide iron(II) clathrochelates to BSA and HSA was studied by CD spectroscopy. These inherently optically inactive cage complexes (Fig. 3a) were found to gain optical activity upon their binding to both given serum albumins, that resulted in an appearance of intense ICD bands in the 350–600 nm range (Fig. 3a and b). These bands correspond to macrobicyclic iron(II) tris-dioximate clathrochelate UV-vis absorption bands (Fig. S4, ESI†), and are assigned to the metal-to-ligand Fed → Lπ* charge transfer transitions in the quasaromatic macrobicyclic frameworks.

The binding to albumins induces CD bands that are distinct for HSA and BSA, in terms of intensity in the case of clathrochelate *meta*-isomer 2, and also in the shape for *ortho*- and *para*-substituted analogs 1 and 3, respectively (Fig. 3a and b). *meta*-Isomer 2 shows a positive-sign ICD band with a maximum at 446 nm and higher intensity of the CD signal. The ICD band of *para*-substituted clathrochelate 3 bound to BSA is less intense, but has a similar shape to that of *meta*-isomer 2 (dominant positive-sign band at 450 nm). In the presence of HSA, the spectrum of *para*-isomer 3 changes its shape exhibiting a “double peak” negative-sign band with the main maximum near 430 nm. The ICD spectrum of *ortho*-substituted clathrochelate 1 in the presence of BSA is of low intensity and located in the negative range; with HSA it is much more intense and contains a negative band with a maximum at 447 nm.

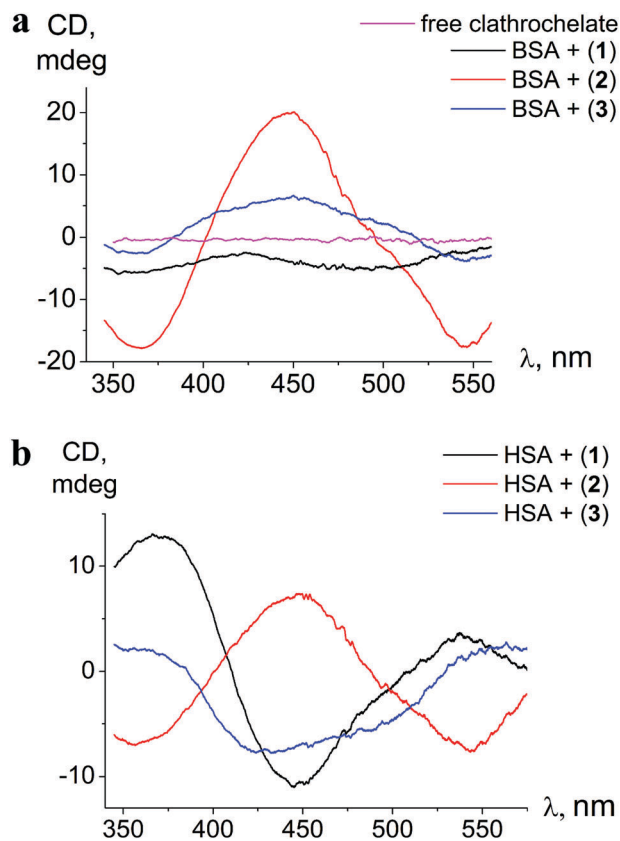


Fig. 3 ICD spectra of clathrochelates 1–3 in the presence of BSA (a) and HSA (b); $C_{\text{albumin}} = 8 \times 10^{-5} \text{ mol l}^{-1}$, $C_{\text{clt}} = 4 \times 10^{-5} \text{ mol l}^{-1}$. Spectra are recorded in 0.05 M Tris HCl pH 7.9.

The intensities of ICD bands of hexa-carboxyl-terminated iron(II) clathrochelates in the presence of BSA are substantially lower than those of their dicarboxyl-terminated analogs reported earlier.³¹ Moreover, for all the di- and mono-substituted carboxyphenylsulfide cage metal complexes the shape of ICD bands in the presence of BSA was similar, with an intense negative maximum at 450 nm.³¹

Hexa-carboxyphenylsulfide iron(II) clathrochelates reveal the ICD sensitivity to related serum albumins, and are capable of discriminating between BSA and HSA hosts, giving different ICD spectra. This spectral discrimination is affected by the constitutional isomerism of the macrobicyclic complexes: it is more pronounced for *ortho*- and *para*-substituted cage complexes, 1 and 3, respectively, and substantially less manifested in the case of *meta*-isomer 2.

The differences in the sequences and thus structures of albumins lead to the alterations of the arrangement of the drug binding sites of BSA and HSA. Hence, variations of ICD outputs of BSA- and HSA-bound hexacarboxy-terminated iron(II) clathrochelates are suggested to be caused by distinct arrangements of BSA- and HSA-clathrochelate assemblies that come from the structural distinctions of BSA and HSA binding sites. The fluorescent data obtained here clearly indicate that the clathrochelate–protein binding is associated with albumin’s drug **site 1**.



3.2. Sensing of albumin conformational transitions by ICD of clathrochelates

To estimate the effect of albumin tertiary structure alterations on the ICD response given by iron(II) clathrochelates, the protein conformation changes were triggered by the variation of pH (Table 1).^{13,52–57} The acidic F-form mainly concerns unfolding of domain III, while in the basic B-form an alteration of the conformation of domain I occurs.⁵³ In the neutral N-form, an interaction between **site 1** and **site 2** is suggested, while in the B-form, the distance between the corresponding subdomains increases and this interaction disappears.⁵⁸

Changes in ICD spectra of the protein–clathrochelate assemblies with pH variations were studied for both albumins. The corresponding fluorescence quenching experiments were performed only for BSA since its intrinsic emission is more affected by assembling with clathrochelate (see Section 3.1.2).

3.2.1. Changes of albumin fluorescence quenching by clathrochelates upon pH variation. A strong influence of media pH on the quenching of BSA fluorescence by the iron(II) clathrochelates was revealed. The most significant quenching effect (15 to 37-fold) was observed at pH 6, where the N-form predominates, while at pH 3.7 (N–F-transition), the effect was negligible (with only up to 1.8-fold quenching). In a slightly basic medium, *i.e.* at pH 7.9 (N–B transition), moderate quenching (about 7-fold) occurred (Fig. 4, 5 and Fig. S5, ESI[†]).

Quenching of BSA intrinsic fluorescence depends on the constitutional isomerism of the iron(II) clathrochelate terminal carboxy groups (Fig. 4, 5 and Fig. S6, ESI[†]). Maximal variation of quenching *versus* pH was observed for *para*-isomer 3 (from 2- to 37-fold, upon the F–N transition and N-forms of BSA, respectively, (Fig. S5, ESI[†])). Also, constitutional isomerism affected the quenching patterns of these cage metal complexes (Fig. S5, ESI[†]).

It has to be mentioned that the pH-dependent experiments were performed in a range of pH that includes the albumin isoelectric point and p*K* of iron(II) clathrochelates. Both proteins have the same isoelectric point with pI about 4.7;^{49,52} p*K* values for the hexacarboxyphenylsulfide cage metal complexes were estimated by potentiometric titrations, and are in the range 5.5–6.3, depending on constitutional isomerism (data not presented).

Processes of dissociation of terminal carboxyl groups of clathrochelates are considered to affect the albumin–clathrochelate non-covalent interactions, leading to strong quenching of Trp fluorescence at pH 6, as compared to pH 3.7. This also indicates the proximity of the guest clathrochelate to a Trp residue in the formed assembly.

Moreover, the small effect of iron(II) clathrochelates on BSA fluorescence in acidic media could be due to the conformation

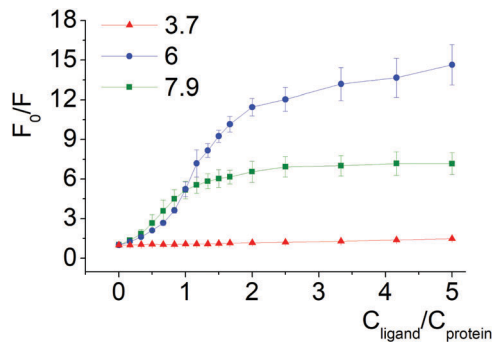


Fig. 4 Stern–Volmer plots of BSA fluorescence quenching by compound 1 at pH 3.7, 6.0 and 7.9.

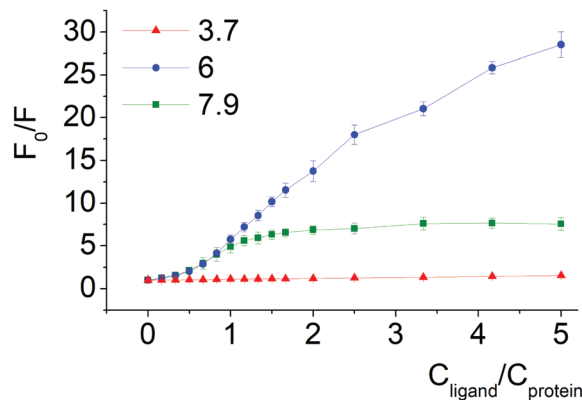


Fig. 5 Stern–Volmer plots of BSA fluorescence quenching by compound 2 at pH 3.7, 6.0 and 7.9.

transition (spatial separation) of the domains III and I (Fig. 2). In the N-form, the binding of the clathrochelate molecule to **site I** (domain I) could be additionally stabilized by spatial interactions with proximal domain III, thus separation of this domain upon the decrease of pH promotes re-arrangement or dissociation of the clathrochelate–protein associate.

3.2.2. Changes of ICD spectra of clathrochelates with pH variation. ICD spectra were recorded for iron(II) clathrochelates in assemblies with BSA and HSA, in pH range 4–9 (Fig. 6a–c and Fig. S5, ESI[†]).

The conformation alterations of a host protein molecule triggered by pH variation cause changes of the ICD spectra of the guest clathrochelate; the changes depend on the origin of serum albumin (BSA or HSA).

In associates with HSA, iron(II) clathrochelates change the shape and intensity of their ICD-bands upon pH variation, indicating rearrangements⁵⁹ of protein–clathrochelate assemblies. The changes were the most pronounced for *meta*-isomer 2 (Fig. 6).

Upon pH-triggered conformational modifications of BSA, the intensity and maxima of ICD-bands of *meta*- and *para*-clathrochelates were changed, while in the case of *ortho*-clathrochelate also the shape of the bands was altered (Fig. 6a, b and Fig. S5, ESI[†]).

In acidic medium (pH 3.7) all iron(II) clathrochelate isomers showed low intensity ICD spectra (up to Δ CD = 2.2 mdeg for

Table 1 Conformations of BSA macromolecule in various pH ranges

Conformer	F (fast)	↔	N (normal)	↔	B (basic)
pH range	2.5–3.5		5–7		9–10
Transition pH		3.5–5		7–9	



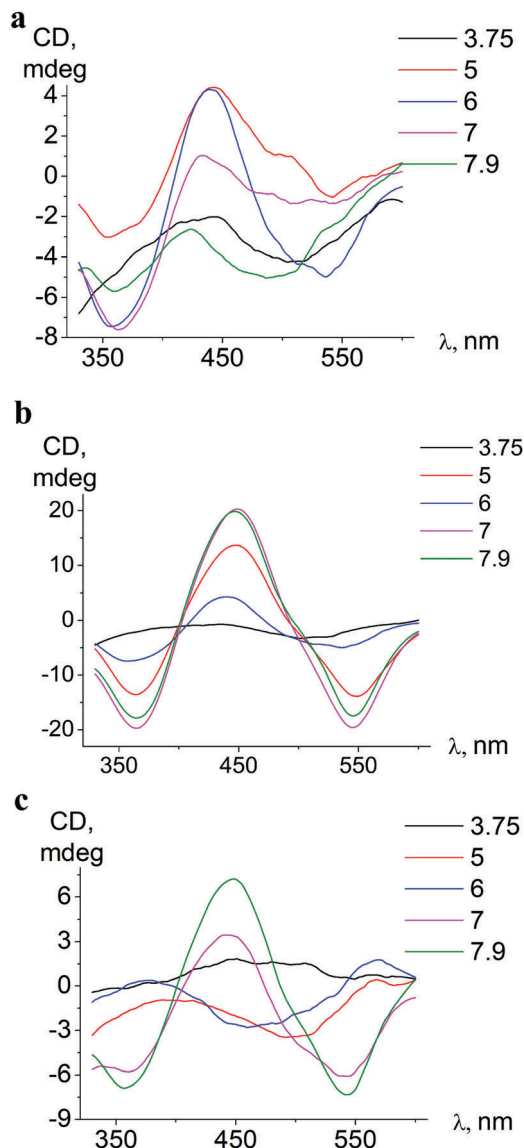


Fig. 6 pH-Dependent ICD spectra of *ortho*-isomer **1** bound to BSA (a), *meta*-isomer **2** bound to BSA (b), and *meta*-isomer **2** bound to HSA (c).

ortho-isomer **1** with BSA); together with a very low albumin fluorescence quenching degree (Fig. 4 and 5) this may evidence clathrochelate–albumin assembly dissociation.

In the pH range 5–9 the bands of ICD spectra of clathrochelate–albumin assemblies are the most intense (Fig. 6a–c and Fig. S5, ESI[†]) and the ability to discriminate between BSA and HSA hosts *via* the difference of ICD signals is the most pronounced. The variations of the ICD spectra probably reflect rearrangement of the albumin–clathrochelate assembly that may occur upon passing through clathrochelate p*K* points (at pH 5.5–6.3), and also at more basic pH (7–8) may be caused by change of protein conformation from the N- towards the B-form.

Thus iron(II) clathrochelates in assemblies with albumin change the shape and intensity of the CD spectra with a variation of the pH of the medium, and consequently with protein tertiary

structure transitions. This points to the high sensitivity of clathrochelate CD output to the arrangement of the structure of their associates with host proteins. Thus, it allows suggesting these cage metal complexes as potential tools for monitoring of protein conformation changes.

3.3. Competitive binding studies using ibuprofen and warfarin as site specific binders

To evaluate the preferable iron(II) clathrochelate binding site in serum albumins, we carried out experiments of clathrochelate displacement by specific binders of albumin sites **1** and **2**, warfarin and ibuprofen, respectively.^{3,13,40} These site-specific binders show high affinity to albumin, with measured binding constants of about $2.5 \times 10^5 \text{ M}^{-1}$ for warfarin,⁶⁰ and $2 \times 10^6 \text{ M}^{-1}$ for ibuprofen.⁶¹ Upon binding to serum albumin, neither warfarin nor ibuprofen exhibit any ICD spectra in the visible spectral range.³ Therefore, evaluation of the iron(II) clathrochelate preference to certain binding sites is performed by monitoring the changes in the ICD spectra of clathrochelate upon the addition of each of these site-specific binders.

For the competitive binding studies on serum albumin with site-specific ligands, the *para*-substituted constitutional isomer **3** was used since it shows the binding ratio 1:1 to albumin (see Section 3.4), and certain specificity to only one of the binding sites could be expected. Generally, an addition of low concentrations of site-specific ligands to the clathrochelate–protein assembly did not influence the clathrochelate ICD output. Only the presence of a high excess of the site-specific binders (from 30-fold excess) resulted in changes of the ICD-band intensity (Fig. 7).

Despite the affinity of the site-specific binders being a few orders of magnitude higher than that determined for clathrochelate **3** ($2.5 \times 10^5 \text{ M}^{-1}$ for warfarin, $2 \times 10^6 \text{ M}^{-1}$ for ibuprofen, over $5.3 \times 10^3 \text{ M}^{-1}$ for **3**, Table 2), only in the case of a 50-fold excess of ibuprofen over the clathrochelate **3**–HSA assembly was a noticeable decrease of the ICD band intensity, up to 2.5-fold, observed (Fig. 7). This indicates that warfarin and ibuprofen displace the iron(II) clathrochelate from its associate with albumin only insignificantly, and thus the competitive binding studies do not provide specific information about the binding site preference.

3.4. Calorimetric study of the supramolecular clathrochelate-to-BSA association

Thermodynamic parameters of supramolecular BSA-to-clathrochelate assemblies were determined using the ITC technique (Fig. 8); the obtained values are summarized in Table 2. The difference between the binding modes of *ortho*- and *meta*-isomers and the *para*-isomer is clearly seen from the shapes of the plots of the binding heat effect *versus* the clathrochelate-to-BSA molar ratio (Fig. 8), as well as from the values of the corresponding thermodynamic parameters (Table 2). Indeed, ΔG values for *meta*- and *ortho*-isomers of clathrochelate complexes are similar, while that for the *para*-substituted cage complex is smaller. According to this, the binding constant values K_a are almost the same for the *ortho*- and *meta*-isomers **1** and **2**



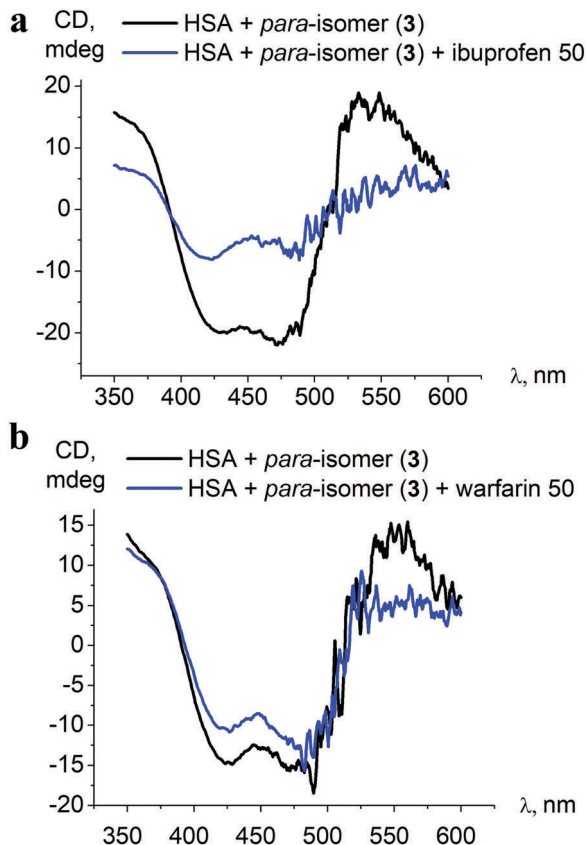


Fig. 7 Initial ICD spectra of the *para*-isomer **3**–HSA assembly and those after addition of a 50-fold excess of albumin site-specific drugs ibuprofen (a) and warfarin (b).

Table 2 Thermodynamic parameters of the supramolecular assembly between BSA and iron(II) clathrochelates

Compound	ΔH^a (kJ mol ⁻¹)	ΔS^a (J mol ⁻¹ K ⁻¹)	ΔG^a (kJ mol ⁻¹)	K_a^b (10 ³ mol l ⁻¹)	n^c
1	-9.1	53.2	-24.9	24	1.95
2	-17.2	27.2	-25.3	28	1.9
3	-23.2	-6.5	-19.3	5.3	0.9

^a ΔH , ΔS and ΔG are the changes of enthalpy, entropy and Gibbs free energy, respectively, upon the binding of clathrochelates to BSA. ^b K_a is a clathrochelate-to-BSA association constant. ^c n is the stoichiometry of the interaction, thus also the calculated number of the clathrochelates molecules per BSA macromolecule as a host. The area under each peak was integrated and fit to an independent binding model to determine the binding affinity (K_a), enthalpy (H) and stoichiometry (n). Since the temperature (T) is held constant throughout, the free energy (ΔG) of the binding reaction can be determined by: $\Delta G = -RT \ln K_a$. ITC directly measures ΔH , so the change in entropy (ΔS) can be determined by: $\Delta S = (\Delta H - \Delta G)/T$. The independent model assumes n -independent binding sites and close thermodynamic parameters of each site. The binding ratio 2:1 was obtained for *ortho*- and *meta*-isomers, thus both isomers bind to BSA with similar K_a .

(2.4×10^4 and 2.8×10^4 M⁻¹, respectively), while for *para*-functionalized compound **3** this value is 5 times lower (5.3×10^3 M⁻¹). These data are in accordance with the results of the fluorescent quenching studies (Fig. 2a and b), where *ortho*- and *meta*-isomers **1** and **2** quench the BSA emission with the same

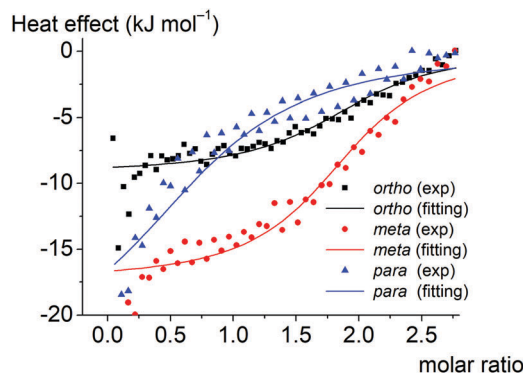


Fig. 8 The experimental (depicted in the points) and fitted (depicted in the solid lines) plots of the binding heat effect versus the BSA-to-clathrochelate molar ratio for the *ortho*-, *meta*- and *para*-substituted hexacarboxyphenyl-terminated iron(II) clathrochelates **1–3** as guests.

intensity, while *para*-isomer **3** demonstrates less intense quenching. Thus, the supramolecular binding of the *ortho*- and *meta*-substituted iron(II) clathrochelates to BSA is suggested to be more favorable as compared to their *para*-isomer **3**.

Enthalpy (ΔH) and entropy (ΔS) changes for these assemblies are also affected by the constitutional isomerism of the iron(II) clathrochelates (Table 2). Both hydrophobic interactions ($\Delta S > 0$) and intermolecular attractions ($\Delta H < 0$) contribute to the binding of the *ortho*- and *meta*-substituted iron(II) cage complexes **1** and **2** to BSA. In the case of their *para*-isomer **3**, we suggest that its assembly with BSA is driven mainly by intermolecular attractions ($\Delta H < 0$), while a contribution of hydrophobic interactions does not exceed the entropy losses caused by the decrease in conformational degrees of freedom upon the corresponding protein-to-clathrochelate supramolecular binding (thus, total $\Delta S < 0$). The influence of hydrophobic effects on binding decreases in the order *ortho* > *meta* > *para*-, while enthalpy effects increase (a predominant role of the energy from non-covalent interactions).

The obtained results can be also explained by the peculiarities of the spatial arrangements of the terminal functionalizing carboxyl groups of the clathrochelate guests. In the case of *para*-isomer **3** of the hexacarboxyphenylsulfide clathrochelate, an external “shell” of the molecule is formed by the “sticking out” terminal polar carboxyl groups, which hampers the ability of this molecule to enter the hydrophobic interactions. In the case of the *ortho*- and *meta*-substituted clathrochelate molecules **1** and **2**, their terminal carboxyl groups are positioned closer to the cage framework, thus making their inclusion into the hydrophobic cavities of protein macromolecules easier and their supramolecular binding is energetically more favorable. As for the enthalpy effect, we suppose that the *para*-isomer **3** has a higher local dipole moment of ribbed substituents as compared to those for *meta*- and *ortho*-substituted analogs **1** and **2**, thus causing an increase in the energy of dipole-dipole interactions.

The number of the iron(II) clathrochelate molecules per BSA macromolecule (n) also depends on their constitutional isomerism. This ratio is estimated as $n = 2$ for the *ortho*- and *meta*-isomers **1** and **2** and $n = 1$ for the *para*-substituted analog **3**. This suggests that one additional site on the BSA globule is



available for the “stable binding” of the *ortho*- and *meta*-substituted clathrochelates. This could be explained by the higher number of geometric configurations of the clathrochelate molecule (*i.e.* the variations of the shape) available due to the rotation of “inherently asymmetric” *ortho*- and *meta*-functionalized ribbed substituents compared to the “inherently symmetric” *para*-functionalized substituents. Higher structural variability allows more flexible tuning of the iron(II) clathrochelate geometry to the shape of the binding site and promotes more precise adsorption of carboxyphenylsulfide groups to the complimentary binding groups of the protein. The independent binding model suggests that two molecules of each clathrochelate isomer bind to albumin with similar K_a . Hence we could consider two “thermodynamically similar” sites on the BSA molecule where *ortho*- and *meta*-isomers are able to bind.

Among studied clathrochelates, the *para*-isomer is the most sensitive to albumin binding site structure distinctions (discriminating HSA and BSA) at neutral and slightly basic pH. This isomer strongly reflects changes that the albumin molecule undergoes when passing from acidic to slightly basic pH, and the quenching of protein fluorescence (*i.e.* effect on the Trp residue) at slightly basic media is most pronounced for this isomer. The clathrochelate-to-albumin binding ratio of 1:1 (established by ITC) and strong effect on protein fluorescence allow suggesting that the exact binding site for this isomer is Sudlow **site 1** of the albumin molecule. Thus, despite the lower binding constant values compared with *ortho*- and *meta*-clathrochelate isomers, the *para*-isomer is considered most suitable as a structure sensitive CD-reporting molecule for albumins.

4. Conclusions

In summary, cage metal complexes iron(II) clathrochelates have shown potency as molecular three-dimensional scaffolds for the design of CD-sensitive reporters able to recognize specific elements of protein surfaces. These important unconventional properties may lead to their possible future use in biochemistry- and medicine-related fields.

Here we show that hexa-carboxyphenylsulfide iron(II) clathrochelates discriminate between proteins of similar structure, in this case HSA and BSA, giving distinct ICD spectra. These cage metal complexes sense the variation of the arrangement of binding sites of these particular proteins. Binding of clathrochelates to **site 1** of albumins is suggested based on protein fluorescence quenching studies.

These iron(II) clathrochelates bound to albumin could reflect the transitions of the protein conformation by the changes of the band profile and intensity of their CD spectra. In this work, such changes of ICD bands were observed together with the variation of medium pH that in turn triggered the alteration of the tertiary structure of albumin.

The above described reporting properties depend on the constitutional isomerism of the ribbed carboxyphenyl substituents and are the most pronounced for the *ortho*- and *para*-isomers of the iron(II) clathrochelate. The *para*-isomer clathrochelate is suggested

as the most appropriate structure-sensitive CD-reporter for albumin studies and discrimination.

The thermodynamic parameters of the clathrochelate-to-BSA assemblies were estimated by ITC, which showed that constitutional isomerism determines the characteristics of such assemblies. Thus *meta*- and *ortho*-isomers have higher binding constants ($K_a \sim 2 \times 10^4 \text{ M}^{-1}$) and clathrochelate-to-albumin binding ratios ($n = 2$) than the *para*-isomer ($K_a \sim 5 \times 10^3 \text{ M}^{-1}$, $n = 1$).

Conflicts of interest

There are no conflicts to declare.

Acknowledgements

The project leading to these results has received funding from the European Union's Horizon 2020 research and innovation programme under the Marie Skłodowska-Curie grant agreement no. 778245. The synthesis of cage complexes was supported by the Russian Science Foundation (grant 16-13-10475).

References

- 1 C. Wolf and K. Bentley, Chirality sensing using stereodynamic probes with distinct electronic circular dichroism output, *Chem. Soc. Rev.*, 2013, **42**, 5408–5424.
- 2 N. Berova, L. Di Bari and G. Pescitelli, Application of electronic circular dichroism in configurational and conformational analysis of organic compounds, *Chem. Soc. Rev.*, 2007, **36**, 914–931.
- 3 D. Venturini, A. de Souza, I. Caracelli, N. Morgon, L. da Silva-Filho and V. Ximenes, Induction of axial chirality in divanillin by interaction with bovine serum albumin, *PLoS One*, 2017, **12**, e0178597.
- 4 F. Zsila, Z. Bikádi, I. Fitos and M. Simonyi, Probing protein binding sites by circular dichroism spectroscopy, *Curr. Drug Discovery Technol.*, 2004, **1**, 133–153.
- 5 Y. Lopukhin, G. Dobretsov and Y. Gryzunov, Conformational changes in albumin molecule: a new response to pathological process, *Bull. Exp. Biol. Med.*, 2000, **130**, 615–619.
- 6 K. Oetl and R. Stauber, Physiological and pathological changes in the redox state of human serum albumin critically influence its binding properties, *Br. J. Pharmacol.*, 2007, **151**, 580–590.
- 7 A. Arasteh, S. Farahi, M. Habibi-Rezaei and A. Moosavi-Movahedi, Glycated albumin: an overview of the *in vitro* models of an *in vivo* potential disease marker, *J. Diabetes Metab. Disord.*, 2014, **13**, 49.
- 8 A. Ivanov, E. Korolenko, E. Korolik, S. Firsov, R. Zhabankov, M. Marchewka and H. Ratajczak, Chronic liver and renal diseases differently affect structure of human serum albumin, *Arch. Biochem. Biophys.*, 2002, **408**, 69–77.
- 9 M. Moergel, P. Kämmerer, K. Schnurr, M. Klein and B. Al-Nawas, Spin electron paramagnetic resonance of albumin for



- diagnosis of oral squamous cell carcinoma (OSCC), *Clin. Oral Investig.*, 2012, **16**, 1529–1533.
- 10 P. Mineo, N. Micali, V. Villari, M. G. Donato and E. Scamporrino, Reading of protein surfaces in the native state at micromolar concentrations by a chirogenetic porphyrin probe, *Chemistry*, 2012, **18**, 12452–12457.
 - 11 D. Tedesco and C. Bertucci, Induced circular dichroism as a tool to investigate the binding of drugs to carrier proteins: classic approaches and new trends, *J. Pharm. Biomed. Anal.*, 2015, **113**, 34–42.
 - 12 M. Nag, K. Bera, S. Chakraborty and S. Basak, Sensing of hydrophobic cavity of serum albumin by an adenosine analogue: fluorescence correlation and ensemble spectroscopic studies, *J. Photochem. Photobiol., B*, 2013, **127**, 202–211.
 - 13 N. Berova, *Comprehensive chiroptical spectroscopy*, Hoboken, NJ, Wiley, 2012, 665–705.
 - 14 F. S. Graciani and V. F. Ximenes, Investigation of human albumin-induced circular dichroism in dansylglycine, *PLoS One*, 2013, **8**, e76849.
 - 15 F. Zsila, T. Imre, P. T. Szabó, Z. Bikádi and M. Simonyi, Induced chirality upon binding of *cis*-parinaric acid to bovine beta-lactoglobulin: spectroscopic characterization of the complex, *FEBS Lett.*, 2002, **520**, 81–87.
 - 16 P. Mineo, N. Micali, V. Villari, M. G. Donato and E. Scamporrino, Reading of protein surfaces in the native state at micromolar concentrations by a chirogenetic porphyrin probe, *Chemistry*, 2012, **18**, 12452–12457.
 - 17 D. N. de Vasconcelos and V. F. Ximenes, Albumin-induced circular dichroism in Congo red: applications for studies of amyloid-like fibril aggregates and binding sites, *Spectrochim. Acta, Part A*, 2015, **150**, 321–330.
 - 18 Y. Z. Voloshin, N. A. Kostromina and R. Kramer, *Clathrochelates: synthesis, structure and properties*, Elsevier Science, Amsterdam, Oxford, 2002.
 - 19 Y. Z. Voloshin, I. Belaya and R. Krämer, *Cage Metal Complexes clathrochelates revisited*, Springer, 2017.
 - 20 S. Tomy, S. I. Shylin, D. Bykov, V. Ksenofontov, E. Gumienna-Kontecka, V. Bon and I. O. Fritsky, Indefinitely stable iron(IV) cage complexes formed in water by air oxidation, *Nat. Commun.*, 2017, **8**, 14099.
 - 21 V. V. Novikov, O. A. Varzatskii, V. V. Negrutska, Y. N. Bubnov, L. G. Palchykovska, I. Y. Dubey and Y. Z. Voloshin, Size matters, so does shape: inhibition of transcription of T7 RNA polymerase by iron(II) clathrochelates, *J. Inorg. Biochem.*, 2013, **124**, 42–45.
 - 22 O. A. Varzatskii, V. V. Novikov, S. V. Shulga, A. S. Belov, A. V. Vologzhanina, V. V. Negrutska, I. Y. Dubey, Y. N. Bubnov and Y. Z. Voloshin, Copper-promoted reductive homocoupling of quasi-aromatic iron(II) clathrochelates: boosting the inhibitory activity in a transcription assay, *Chem. Commun.*, 2014, **50**, 3166–3168.
 - 23 O. A. Varzatskii, S. V. Shul'ga, A. S. Belov, V. V. Novikov, A. V. Dolganov, A. V. Vologzhanina and Y. Z. Voloshin, Copper(I)- and copper(0)-promoted homocoupling and homocoupling-hydrodehalogenation reactions of dihalogenoclathrochelate precursors for C–C conjugated iron(II) bis-cage complexes, *Dalton Trans.*, 2014, **43**, 17934–17948.
 - 24 A. Belov, A. Vologzhanina, V. Novikov, V. Negrutska, I. Dubey, Z. A. Mikhailova, E. G. Lebed and Y. Voloshin, Synthesis of the first morpholine-containing iron(II) clathrochelates: a new class of efficient functionalized transcription inhibitors, *Inorg. Chim. Acta*, 2014, **421**, 300–306.
 - 25 O. A. Varzatskii, A. V. Vologzhanina, V. V. Novikov, S. V. Vakarov, R. V. Oblap and Y. Z. Voloshin, Inhibition of DNA synthesis in the transcription system of Taq DNA polymerase by various iron and cobalt(II) tris-dioximate clathrochelates: *in vitro* study and X-ray structure of leader inhibitors, the carboxyl-terminated macrobicyclic complexes, *Inorg. Chim. Acta*, 2018, **482**, 90–98.
 - 26 V. Kovalska, S. Chernii, V. Cherepanov, M. Losytskyy, V. Chernii, O. Varzatskii, A. Naumovets and S. Yarmoluk, The impact of binding of macrocyclic metal complexes on amyloid fibrillization of insulin and lysozyme, *J. Mol. Recognit.*, 2017, **30**, e2622.
 - 27 V. Kovalska, V. Cherepanov, M. Losytskyy, S. Chernii, A. Senenko, V. Chernii, I. Tretyakova, S. Yarmoluk and S. Volkov, Anti-fibrillogenic properties of phthalocyanines: effect of the out-of-plane ligands, *Bioorg. Med. Chem.*, 2014, **22**, 6918–6923.
 - 28 Y. Voloshin, V. Novikov and Y. Nelyubina, Recent advances in biological applications of cage metal complexes, *RSC Adv.*, 2015, **5**, 72621–72637.
 - 29 V. B. Kovalska, M. Y. Losytskyy, S. V. Chernii, V. Y. Chernii, I. M. Tretyakova, S. M. Yarmoluk and S. V. Volkov, Towards the anti-fibrillogenic activity of phthalocyanines with out-of-plane ligands: correlation with self-association proneness, *Biopolym. Cell*, 2013, **29**, 473–479.
 - 30 M. Y. Losytskyy, V. B. Kovalska, O. A. Varzatskii, A. M. Sergeev, S. M. Yarmoluk and Y. Z. Voloshin, Interaction of the iron(II) cage complexes with proteins: protein fluorescence quenching study, *J. Fluoresc.*, 2013, **23**, 889–895.
 - 31 V. B. Kovalska, S. V. Vakarov, M. V. Kuperman, M. Y. Losytskyy, E. Gumienna-Kontecka, Y. Z. Voloshin and O. A. Varzatskii, Induced chirality of cage metal complexes switched by their supramolecular and covalent binding, *Dalton Trans.*, 2018, **47**, 1036–1052.
 - 32 S. V. Vakarov, M. V. Kuperman, V. B. Kovalska and O. A. Varzatskii, Functionalization of the Fe(II) clathrochelates and the effect of the modification on their binding to albumins, *Ukr. Chem. J.*, 2015, **81**, 116–120.
 - 33 S. van Dun, C. Ottmann, L.-G. Milroy and L. Brunsveld, Supramolecular chemistry targeting proteins, *J. Am. Chem. Soc.*, 2017, **139**, 13960–13968.
 - 34 S. H. Hewitt and A. J. Wilson, Metal complexes as “protein surface mimetics”, *Chem. Commun.*, 2016, **52**(63), 9745–9756.
 - 35 I. Belaya, G. Zelinskii, A. Belov, O. Varzatskii, V. Novikov, Y. Z. Voloshin, A. Dolganov, H. Kozłowski, Ł. Szyrwił, Y. Bubnov and Y. Voloshin, Synthesis, spectra and properties of the first protono- and ionogenic tris-dioximate iron(II) clathrochelates, *Polyhedron*, 2012, **40**, 32–39.
 - 36 J. R. Lakowicz, *Principles of fluorescence spectroscopy*, Kluwer Academic/Plenum, New York, London, 2nd edn, 1999.



- 37 Q. Gu and J. E. Kenny, Improvement of inner filter effect correction based on determination of effective geometric parameters using a conventional fluorimeter, *Anal. Chem.*, 2009, **81**, 420–426.
- 38 B. Birdsall, R. W. King, M. R. Wheeler, C. A. Lewis, S. R. Goode, R. B. Dunlap and G. Roberts, Correction for light absorption in fluorescence studies of protein–ligand interactions, *Anal. Biochem.*, 1983, **132**, 353–361.
- 39 M. Kubista, R. Sjöback, S. Eriksson and B. Albinsson, Experimental correction for the inner-filter effect in fluorescence spectra, *Analyt.*, 1994, **119**, 417–419.
- 40 S. S. Sur, L. D. Rabbani, L. Libman and E. Breslo, Fluorescence studies of native and modified neurophysins. Effects of peptides and pH, *Biochemistry*, 1979, **18**, 1026–1036.
- 41 S. Patel, K. K. Sharma and A. Datta, Competitive binding of Chlorin p6 and Dansyl-L-Proline to Sudlow's site II of human serum albumin, *Spectrochim. Acta, Part A*, 2015, **138**, 925–931.
- 42 K. A. Majorek, P. J. Porebski, A. Dayal, M. D. Zimmerman, K. Jablonska, A. J. Stewart, M. Chruszcz and W. Minor, Structural and immunologic characterization of bovine, horse, and rabbit serum albumins, *Mol. Immunol.*, 2012, **52**, 174–182.
- 43 J. Ghuman, P. A. Zunszain, I. Petitpas, A. A. Bhattacharya, M. Otagiri and S. Curry, Structural basis of the drug-binding specificity of human serum albumin, *J. Mol. Biol.*, 2005, **353**, 38–52.
- 44 K. M. Sand, M. Bern, J. Nilsen, H. T. Noordzij, I. Sandlie and J. T. Andersen, Unraveling the interaction between FcRn and albumin: opportunities for design of albumin-based therapeutics, *Front. Immunol.*, 2014, **5**, 682.
- 45 S. Curry, H. Mandelkew, P. Brick and N. Franks, Crystal structure of human serum albumin complexed with fatty acid reveals an asymmetric distribution of binding sites, *Nat. Struct. Biol.*, 1998, **5**, 827–835.
- 46 Y. Akdogan, J. Reichenwallner and D. Hinderberger, Evidence for water-tuned structural differences in proteins: an approach emphasizing variations in local hydrophilicity, *PLoS One*, 2012, **7**, e45681.
- 47 M. Poór, Y. Li, G. Matisz, L. Kiss, S. Kunsági-Máté and T. Koszegi, Quantitation of species differences in albumin–ligand interactions for bovine, human and rat serum albumins using fluorescence spectroscopy: a test case with some Sudlow's site I ligands, *J. Lumin.*, 2014, **145**, 767–773.
- 48 N. Morade, M. R. Ashrafi-Kooshk, S. Ghobadi, M. Shahlaei and R. Khodarahmi, Spectroscopic study of drug-binding characteristics of unmodified and pNPA-based acetylated human serum albumin: Does esterase activity affect micro-environment of drug binding sites on the protein?, *J. Lumin.*, 2015, **160**, 351–361.
- 49 L. Stella, A. L. Capodilupo and M. Bietti, A reassessment of the association between azulene and [60]fullerene. Possible pitfalls in the determination of binding constants through fluorescence spectroscopy, *Chem. Commun.*, 2008, 4744–4746.
- 50 D. C. Carter and J. X. Ho, Structure of serum albumin, *Adv. Protein Chem.*, 1994, **45**, 153–203.
- 51 A. Sułkowska, M. Maciążek-Jurczyk, B. Bojko, J. Równicka, I. Zubik-Skupieć, E. Temba, D. Pentak and W. W. Sułkowski, Competitive binding of phenylbutazone and colchicine to serum albumin in multidrug therapy: a spectroscopic study, *J. Mol. Struct.*, 2008, **881**, 97–106.
- 52 P. J. Sadler and A. Tucker, pH-induced structural transitions of bovine serum albumin. Histidine pKa values and unfolding of the N-terminus during the N to F transition, *Eur. J. Biochem.*, 1993, **212**, 811–817.
- 53 N. El Kadi, N. Taulier, J. Y. Le Huérou, M. Gindre, W. Urbach, I. Nwigwe, P. C. Kahn and M. Waks, Unfolding and refolding of bovine serum albumin at acid pH: ultrasound and structural studies, *Biophys. J.*, 2006, **91**, 3397–3404.
- 54 B. Ahmad, S. Parveen and R. H. Khan, Effect of albumin conformation on the binding of ciprofloxacin to human serum albumin: a novel approach directly assigning binding site, *Biomacromolecules*, 2006, **7**, 1350–1356.
- 55 M. Dockal, D. C. Carter and F. Rüker, Conformational transitions of the three recombinant domains of human serum albumin depending on pH, *J. Biol. Chem.*, 2000, **275**, 3042–3050.
- 56 M. Amiri, K. Jankeje and J. R. Albani, Characterization of human serum albumin forms with pH. Fluorescence lifetime studies, *J. Pharm. Biomed. Anal.*, 2010, **51**, 1097–1102.
- 57 A. Del Giudice, C. Dicko, L. Galantini and N. V. Pavel, Time-Dependent pH Scanning of the Acid-Induced Unfolding of Human Serum Albumin Reveals Stabilization of the Native Form by Palmitic Acid Binding, *J. Phys. Chem. B*, 2017, **121**, 4388–4399.
- 58 K. Yamasaki, T. Maruyama, K. Yoshimoto, Y. Tsutsumi, R. Narazaki, A. Fukuhara, U. Kragh-Hansen and M. Otagiri, Interactive binding to the two principal ligand binding sites of human serum albumin: effect of the neutral-to-base transition, *Biochim. Biophys. Acta*, 1999, **1432**, 313–323.
- 59 Z. Ferenc, Z. Bikádi and M. Simonyi, Circular dichroism spectroscopic studies reveal pH dependent binding of curcumin in the minor groove of natural and synthetic nucleic acids, *Org. Biomol. Chem.*, 2004, **2**, 2902–2910.
- 60 J. Wilting, W. F. van der Giesen, L. H. Janssen, M. M. Weideman, M. Otagiri and J. H. Perrin, The effect of albumin conformation on the binding of warfarin to human serum albumin. The dependence of the binding of warfarin to human serum albumin on the hydrogen, calcium, and chloride ion concentrations as studied by circular dichroism, fluorescence, and equilibrium dialysis, *J. Biol. Chem.*, 1980, **255**, 3032–3037.
- 61 S. Evoli, D. L. Mobley, R. Guzzi and B. Rizzuti, Multiple binding modes of ibuprofen in human serum albumin identified by absolute binding free energy calculations, *Phys. Chem. Chem. Phys.*, 2016, **18**, 32358–32368.

